High-Temperature Transformations in Calcium Orthovanadate Studied with Raman Scattering

Andrzej Grzechnik

École Normale Supérieure de Lyon, 46, allée d'Italie, 69364 Lyon Cedex 07, France

Received August 20, 1997. Revised Manuscript Received February 6, 1998

Raman spectra of $Ca_3(VO_4)_2$ calcium orthovanadate ($R3c$ space group), a high temperature ferroelectric with $T_c = 1383$ K, are analyzed up to 1483 K with a group theory approach and discussed in relation to Raman spectra of other compounds with the palmierite structure ($R\bar{3}m$ space group). The ferroelectric-paraelectric phase transition at $T_c = 1383$ K is interpreted as due to the $R3c \rightarrow R\bar{3}m$ structural transformation. At the 500−800 K temperature range, there occurs a transition to an intermediate between the $R\bar{3}m$ and $R3c$ phases, with all the VO_4^{3-} ions at sites with 3-fold symmetry. There is no soft-mode behavior observed up to 1483 K, suggesting an order−disorder character of the transitions.

Introduction

Calcium orthovanadate, $Ca_3(VO_4)_2$, is a high temperature ferroelectric with $T_c = 1383$ K,[1−4] and it has additional anomalies in dielectric properties[1] and electronic thermal emission spectra[3] at the 550−800 K temperature range. This material is also a luminophor when in solid solution series with other orthovanadates and phosphates, doped with rare-earth elements.[3,5−8] Brixner and Fluornoy[5] studied the properties of $Ca_3(VO_4)_2$ as a possible laser host. The defect structure of this compound along with the presence of V^{4+} ions or rare earth doping accounts for its high electronic conductivity.[9−11]

The crystal structure of $Ca_3(VO_4)_2$ ($R3c$ space group, $Z = 7$)[12] is a distorted variant of the $K_2Pb(SO_4)_2$ palmierite structure ($R\bar{3}m$ space group, $Z = 1$), taken by the whole family of the $Me_3(XO_4)_2$ compounds (Me^{2+}: Sr, Ba, Pb; X^{5+}: P, As, V, Mn).[3,13−18] The ideal structure is comprised of $[Me_{(1)}(XO_4)_2]^{4-}$ layers linked into a crystal network by $Me_{(2)}^{2+}$ cations. The unit cell in $Ca_3(VO_4)_2$, which is isotypic with β-$Ca_3(PO_4)_2$[19,20] and $Ca_3(AsO_4)_2$,[21] is doubled along the a and c axes as a result of displacements of oxygen and calcium atoms from their ideal positions.

Structural transformations in $Ca_3(VO_4)_2$, associated with the dielectric and electronic anomalies at the 550−800 K temperature range and the ferroelectric phase transition at $T_c = 1383$ K, have not been studied extensively so far. Brillouin scattering measurements have revealed no anomalous changes in the elastic constants up to 840 K.[22] In this study, the Raman spectrum of $Ca_3(VO_4)_2$ at room temperature is discussed in relation to the ideal ($R\bar{3}m$) and distorted ($R3c$) palmierite structures and analyzed with a group theory approach. The high-temperature structural changes in this material are subsequently studied with in situ high-temperature Raman scattering up to 1483 K and compared to transformations in other palmierite-type materials.

Experimental Section

The polycrystalline sample of $Ca_3(VO_4)_2$ (a melting point[3] $T_m = 1653$ K) was prepared from a 3:1 mixture of $CaCO_3$ and V_2O_5 (both from Aldrich) melted in a platinum crucible and cooled to room temperature from 1900 K in a modified Deltech furnace (an average cooling rate of 100 K/s). The size of crystallites was about 5−30 μm, as observed under an optical microscope. The phase purity of the product was verified with X-ray diffraction (JCPDS-ICDD No. 39-90).

Unpolarized Raman spectra, with spectral resolution of about 2 cm^{-1}, were collected with a XY Dilor Raman spectrometer (1800 groove/mm gratings) in backscattering geometry with CCD signal detection. Raman scattering was excited

(1) Glass, A. M.; Abrahams, S. C.; Ballmann, A. A.; Loiacono, G. *Ferroelectrics* **1978**, *17*, 579.
(2) Haussühl, S.; Liebertz, J. *Z. Kristallogr.* **1978**, *148*, 87.
(3) Fotiev, A. A.; Trunov, B. K.; Zhuravlev,V. D. *Vanadates of Divalent Metals* (in Russian); Nauka: Moscow, 1985.
(4) Diouri, M.; Drache, M.; Thomas, D. *Rev. Chim. Miner.* **1986**, *23*, 746.
(5) Brixner, L. H.; Flournoy, P. A. *J. Electrochem. Soc.* **1965**, *112*, 303.
(6) Khodos, M. Ya.; Leonidov, I. A.; Fotiev, A. A. *Russ. J. Inorg. Chem.* **1984**, *29*, 1363.
(7) Li, C. Z.; Yang, W. H.; Chang, Y. C. *Ferroelectrics* **1993**, *142*, 131.
(8) Zhuravlev, V. D.; Fotiev, A. A.; Shulgin, B. V. *Izv. Akad. Nauk SSSR Neorg. Mater.* **1979**, *15*, 2003.
(9) Leonidov, I. A.; Fotiev, A. A.; Khodos, M. Ya. *Izv. Akad. Nauk SSSR Neorg. Mater.* **1987**, *23*, 127.
(10) Leonidov, I. A.; Khodos, M. Ya.; Fotiev, A. A. *Izv. Akad. Nauk SSSR Neorg. Mater.* **1988**, *24*, 97.
(11) Leonidov, I. A.; Khodos, M. Ya.; Fotiev, A. A.; Zhukovskaya, A. S. *Izv. Akad. Nauk SSSR Neorg. Mater.* **1988**, *24*, 347.
(12) Gopal, R.; Calvo, C. *Z. Kristallogr.* **1973**, *137*, 67.
(13) Durif, A. *Acta Crystallogr.* **1959**, *12*, 420.
(14) Tarte, P.; Thelen, I. *Spectrochim. Acta A* **1972**, *28*, 5.
(15) Baran, E. J.; Aymonino, P. J. *J. Mol. Struct.* **1970**, *11*, 453.
(16) Carrillo-Cabrera, W.; von Schnering, H. G. *Z. Kristallogr.* **1993**, *205*, 271.
(17) Bachmann, H. G.; Kleber, W. *Fortschr. Mineral.* **1953**, *31/32*, 9.
(18) Süsse, P.; Buerger, M. J. *Z. Kristallogr.* **1970**, *134*, 161.
(19) Dickens, B.; Schroeder, L. W.; Brown, W. E. *J. Solid State Chem.* **1974**, *10*, 232.
(20) de Aza, P. N.; Santos, C.; Pazo, A.; de Aza, S.; Cuscó, R.; Artús, L. *Chem. Mater.* **1997**, *9*, 912.
(21) Baran, E. J. *Z. Anorg. Allg. Chem.* **1976**, *427*, 131.
(22) Congzhou, L.; Yingchuan, C.; Yifeng, Y. *Ferroelectrics* **1990**, *101*, 207.

S0897-4756(97)00581-4 CCC: $15.00
Published on Web 04/01/1998

using an Ar^+ laser at a wavelength of 514.5 nm. The laser power at the sample was about 2 mW to minimize sample heating by the laser irradiation (the actual sample heating by laser irradiation was not measured in this study). High-temperature experiments were carried out with a LINKAM TS-1500 heating stage up to 1483 K. A very thin sample (about 200 μm in thickness and about 2 mm^2 in area) was placed on a sapphire disk (500 μm in thickness) directly over the heating stage thermocouple. The temperature between the measurements was increased with a rate of 10 K/min. The temperature variation during Raman signal collection did not exceed ±5 K in the entire temperature range studied here.

For the measurements at temperatures above 1173 K, it was necessary to account for thermal emission of the sample. At these temperatures the emission spectra were superimposed on the collected Raman signal. Thus, for each temperature above 1173 K, the Raman signal and thermal emission spectrum (i.e., with and without the laser beam for Raman scattering excitation, respectively) were measured under exactly the same experimental conditions (300 s/spectrum). Subsequently, for each temperature, the thermal emission spectrum was subtracted from the recorded Raman signal to obtain the true high-temperature Raman spectrum. The obtained spectra were analyzed with a multiple Lorentzian function and a Lorentzian-type line shape for the Rayleigh elastic scattering. The fitting procedure was described by Yuzyuk et al.[23]

Symmetry Analysis

In the ideal palmierite structure ($R\bar{3}m$ space group, $Z = 1$), the VO_4^{3-} tetrahedra occupy the C_{3v} sites.[16,18] The coordination of intralayer $Me_{(1)}^{2+}$ cations in the $[Me_{(1)}(XO_4)_2]^{4-}$ layers can be described as either octahedral or distorted 12-fold icosahedral one (D_{3d} sites). The coordination number of the interlayer $Me_{(2)}^{2+}$ ions is 10 (C_{3v} sites). The unit cell of $Ca_3(VO_4)_2$ is doubled along the *a* and *c* axes (*R*3*c* space group, $Z = 7$) as a result of displacements of oxygen and calcium atoms from their ideal positions.[12] VO_4^{3-} tetrahedra occupy one C_3 and two C_1 sites, with different tilting perpendicular to the *c* axis. Coordination numbers of two nonequivalent $Ca_{(1)}^{2+}$ cations are 6 (C_3 sites) and 8 (C_1 sites). Three nonequivalent $Ca_{(2)}$ atoms are 6-fold (C_3 sites), 7-fold (C_1 sites), and 8-fold coordinated (C_1 sites). The interlayer $Ca_{(2)}^{2+}$ cations at the C_3 sites are half-occupied with random distribution of vacancies. It additionally leads to the loss of one formula unit per cell along the *c* axis ($Z = 7$).

The internal vibrational modes of the free tetrahedral molecule with T_d symmetry are classified as ν_1 (the symmetric stretching mode of the A_1 symmetry type), ν_2 (the bending mode of the E symmetry type), ν_3 (the antisymmetric stretching mode of the F_2 symmetry type), and ν_4 (the bending mode of the F_2 symmetry type). The descent of symmetry to C_{3v}, C_3, or C_1 subgroups of the T_d supergroup leads to the removal of the degeneracy. For the crystal structures that are related to each other or inferred from each other, it is useful to carry out the group analysis of the optically active vibrational modes in order to elucidate the mechanism of possible phase transitions between them. As indicated by Gopal and Calvo,[12] the hypothetical nondistorted α-$Ca_3(VO_4)_2$ is isostructural with $Ba_3(VO_4)_2$ and $Sr_3(VO_4)_2$ ($R\bar{3}m$).

(23) Yuzyuk, Yu.I.; Gregora, I.; Vorlicek, V.; Petzelt, J. *J. Phys.: Condens. Matter* **1996**, *8*, 619.

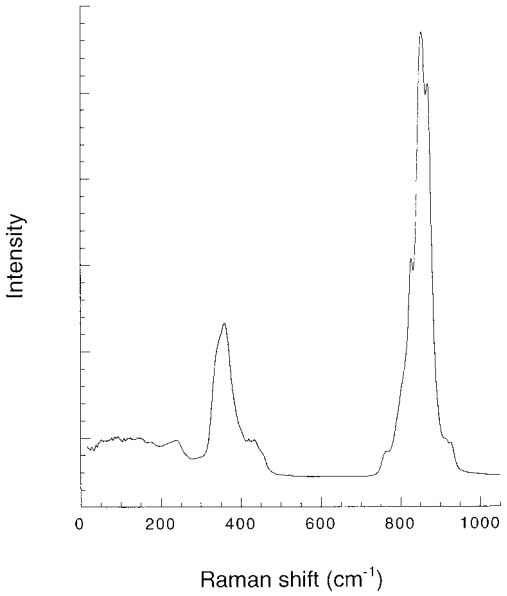

Figure 1. Raman spectrum of $Ca_3(VO_4)_2$ at room temperature.

Group analysis of the normal modes in the ideal palmierite structure ($R\bar{3}m$ space group, $Z = 1$) predicts the following selection rules: $\Gamma_{vib} = 5A_{1g} + A_{2g} + 6E_g + A_{1u} + 5A_{2u} + 6E_u$, where A_{1g} and E_g modes are Raman active and A_{2u} and E_u modes are infrared active.[24,25] Internal stretching and bending VO_4^{3-} modes are distributed as $\Gamma_{int} = 3A_{1g} + 3E_g + 3A_{2u} + 3E_u$, whereas the translational and rotational modes are $\Gamma_T = 2A_{1g} + 2E_g + 2A_{2u} + 2E_u$ and $\Gamma_R = A_{2g} + E_g + A_{1u} + E_u$, respectively. The coupled internal ν_1, ν_2, ν_3, and ν_4 modes of the two distorted tetrahedral VO_4^{3-} ion have $A_{1g} + A_{2u}$, $E_g + E_u$, $A_{1g} + E_g + A_{2u} + E_u$, and $A_{1g} + E_g + A_{2u} + E_u$ symmetry types, respectively.

Analysis of the normal modes in $Ca_3(VO_4)_2$ (*R*3*c* space group, $Z = 7$), assuming random distribution of vacancies at the C_3 sites occupied by interlayer $Ca_{(2)}$ atoms,[12] leads to the following selection rules $\Gamma_{vib} = 44A_1 + 46A_2 + 90E$, where the A_1 and E modes are both infrared and Raman active, while the A_2 modes are optically inactive. Internal stretching and bending VO_4^{3-} modes are distributed as $\Gamma_{int} = 21A_1 + 21A_2 + 42E$, whereas the translational (Γ_T) and rotational (Γ_R) modes are $\Gamma_T = 16A_1 + 18A_2 + 34E$ and $\Gamma_R = 7A_1 + 7A_2 + 14E_2$. The internal ν_1, ν_2, ν_3, and ν_4 modes have $3A_1 + 3A_2 + 4E$, $4A_1 + 4A_2 + 10E$, $7A_1 + 7A_2 + 14E$, and $7A_1 + 7A_2 + 14E$ symmetry types, respectively. The distribution of the internal modes originating from VO_4^{3-} ions at the C_3 sites is $\nu_1 \rightarrow A_1 + A_2$, $\nu_2 \rightarrow 2E$, $\nu_3 \rightarrow A_1 + A_2 + 2E$, and $\nu_4 \rightarrow A_1 + A_2 + 2E$. Similarly, all the internal modes from two nonequivalent VO_4^{3-} ions at the C_1 sites are $\nu_1 \rightarrow 2A_1 + 2A_2 + 4E$, $\nu_2 \rightarrow 4A_1 + 4A_2 + 8E$, $\nu_3 \rightarrow 6A_1 + 6A_2 + 12E$, and $\nu_4 \rightarrow 6A_1 + 6A_2 + 12E$.

Results and Discussion

The first-order Raman spectrum of $Ca_3(VO_4)_2$ taken at room temperature is shown in Figure 1 and wavenumbers of the observed bands are listed in Table 1.

(24) Grzechnik, A.; McMillan, P. F. *Solid State Commun.* **1997**, *102*, 569.

(25) Grzechnik, A.; McMillan, P. F. *J. Solid State Chem.* **1997**, *132*, 156.

Table 1. Observed Optical Phonons (cm^{-1} units) in $Ca_3(VO_4)_2$ at Room Temperature

single crystal[26]			
$A_1 + E^a$	A_1	E	polycrystalline sample
	929		927
916		917	915
		890	
870	870		868
854			853
828	827		827
		808	803
800	792	800	789
760	760	766	764
	455		
		449	450
434			435
			419
400	400	400	398
358	361	361	360
337	337	337	346
297			294
286			
	267	267	
239			242
		223	220
205			
186		183	
176			174
	164		163
		153	154
145			
118	116	116	123
95		94	94
78		77	
66	65	65	
58		54	60
45	47		

[a] Unpolarized.

The band at about 419 cm^{-1} in the Raman spectra recorded from a polycrystalline sample (Table 1) was not observed in single crystal measurements[26] but was detected in the polycrystalline Raman spectrum by Baran.[21] The above symmetry analysis of optically active modes in $Ca_3(VO_4)_2$ demonstrates the complexity of the expected vibrational spectra due to lowering of symmetry from $R\bar{3}m$ to $R3c$, as described by Gopal and Calvo.[12] The number of the observed Raman modes in both single crystal and polycrystalline samples is much smaller (Table 1) than that predicted by symmetry considerations ($44A_1 + 90E$). The symmetry of $R3c$ space group for ferroelectric $Ca_3(VO_4)_2$[1,12] implies that the splittings of the transverse and longitudinal optical modes should be observed in the Raman spectrum, as is the case for $LiNbO_3$ and $LiTaO_3$ with the same space group at room temperature.[27−30] However, such splittings were not identified in the polarized Raman measurements on single crystals.[26]

These observations can be rationalized by a close examination of the crystal structure of $Ca_3(VO_4)_2$ in relation to its vibrational features. Disordering of the nonequivalent oxygen atoms with different local coordination spheres leads to an overlap of many of the predicted modes that would otherwise be split in the case when the vacancies were ordered. Such disordering may influence the coupling of the internal modes of the VO_4^{3-} ions and broadening of the observed Raman bands at room temperature (Figure 1). It indicates that, unlike in $Sr_3(VO_4)_2$ and $Ba_3(VO_4)_2$,[24,25] strict analysis and assignment of the observed Raman bands in $Ca_3(VO_4)_2$ in terms of the VO_4^{3-} internal ν_1, ν_2, ν_3, and ν_4 modes as well as VO_4^{3-} external and cation oscillations, presented previously,[21,26,31,32] may not be valid. Second, there are 14 VO_4^{3-} ions in the unit cell[12]—two equivalent ions at the C_3 sites, and six equivalent ions at the two nonequivalent C_1 sites, each. From the vibrational spectroscopy point of view, it should result in the coupling of the same modes of the equivalent VO_4^{3-} ions in the crystal lattice because of the conjugated excitations of the internal modes.[20] Additionally, the intense bands in the low-wavenumber region (Figure 1), which one would tend to assign to the O−V−O bending modes, have a large contribution from the oscillators of intra- and interlayer Ca^{2+} cations due to the relatively low atomic mass of the calcium atoms and disordering of the structure. To illustrate this point, the work by Kristallov and Fotiev should be recalled.[31] They carried out a valence force field calculation of the optical modes in $Ca_3(VO_4)_2$ without taking into account any observed Raman modes below about 300 cm^{-1} and without including any terms due to the Ca oscillations in their proposed force field. As a consequence, their assignment of the calculated bands to symmetry types of the optically active modes is different from the results of the polarized Raman measurements on a single crystal[26] (Table 1). Recently, it was found in the study of the high-pressure behavior of $Ca_3(VO_4)_2$[33] that the bands at 294, 220, 163, and 123 cm^{-1} have very large microscopic Grüneisen parameters, related to the pressure dependence of the unit-cell volume. Accordingly, these bands are assigned primarily to the $Ca_{(2)}^{2+}$ displacements perpendicular to the c axis, along which compressibility is much higher than the one along the a axis.

The comparison of the first-order Raman spectra of $Ca_3(VO_4)_2$ and β-$Ca_3(PO_4)_2$, two isotypic compounds,[12,19] needs some consideration. The observed Raman bands in $Ca_3(VO_4)_2$ (Figure 1 and Table 1) are distributed only in two wavenumber regions corresponding to the V−O stretching modes (950−750 cm^{-1}) and O−V−O bending modes mixed with the translational and rotational modes of the VO_4^{3-} groups as well as Ca^{2+} cation displacements (450−50 cm^{-1}). The Raman bands in β-$Ca_3(PO_4)_2$[20] are distributed in five distinct 170−305, 405−483, 547−631, 946−970, and 1005−1091 cm^{-1} wavenumber ranges, corresponding to the lattice modes, ν_2, ν_4, ν_1, and ν_3 internal modes of the PO_4^{3-} ions, respectively. These differences between $Ca_3(VO_4)_2$ and β-$Ca_3(PO_4)_2$ can be assigned not only to the differences in atomic masses of the V and P atoms but also to the larger bond length and angle distortions of the tetrahedral units in the structure of β-$Ca_3(PO_4)_2$.[12,19]

Raman spectra recorded upon heating from room temperature to 1483 K, along with the temperature shift

(26) Li, C. Z; Yang, W. H.; Chang, Y. C. *Jap. J. Appl. Phys.* **1985**, *24* (Suppl. 24-2), 508.
(27) Barker, A. S.; Loudon, R. *Phys. Rev.* **1967**, *158*, 433.
(28) Johnson, W. D.; Kaminov, I. P. *Phys. Rev.* **1968**, *168*, 1045.
(29) Tezuka, Y.; Shin, S.; Ishigame, M. *Phys. Rev. B* **1994**, *49*, 9312.
(30) Grzechnik, A.; McMillan, P. F. *J. Phys. Chem. Solids* **1997**, *58*, 1071.
(31) Kristallov, L. V.; Fotiev, A. A. *Russian J. Inorg. Chem.* **1981**, *26*, 1456.
(32) Porotnikov, N. V.; Burneiko, O. A.; Krasnenko, T. I.; Fotiev, A. A. *Russ. J. Inorg. Chem.* **1993**, *38*, 1365.
(33) Grzechnik, A. *J. Solid State Chem.*, submitted.

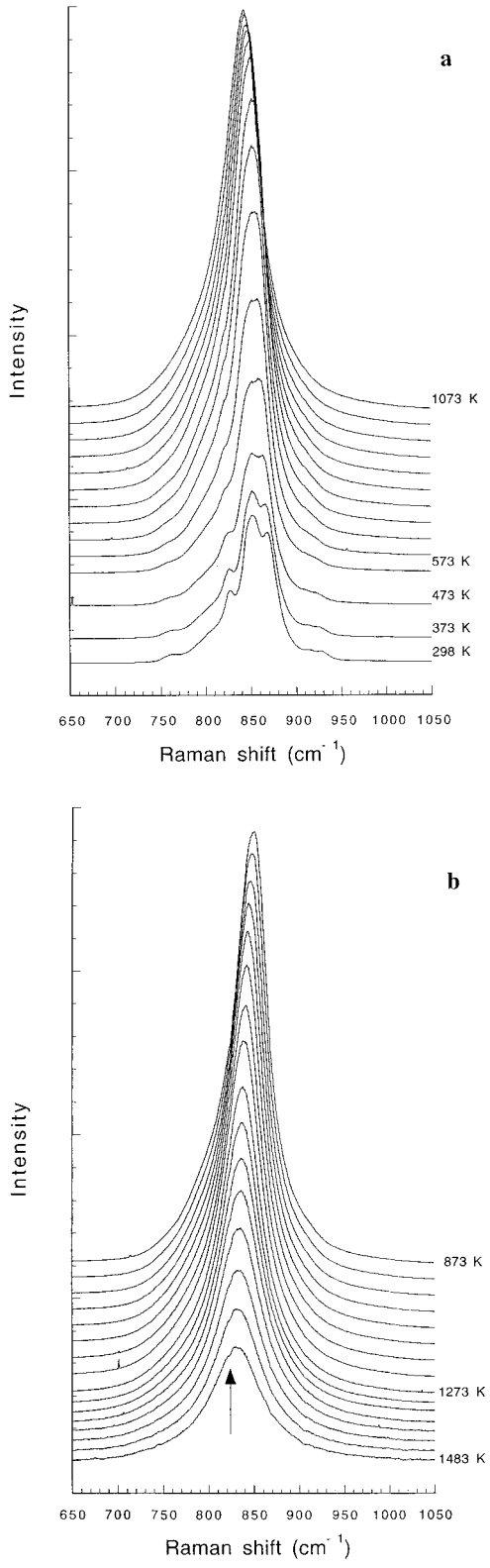

Figure 2. Raman spectra of $Ca_3(VO_4)_2$, corrected for thermal emission, in the high-wavenumber region as a function of temperature: (a) 298−1073 K; (b) 873−1483 K. The spectra in the 573−1273 and 1273−1483 K temperature ranges were collected every 50 and 30 K, respectively. The arrow indicates an artifact due to the detector.

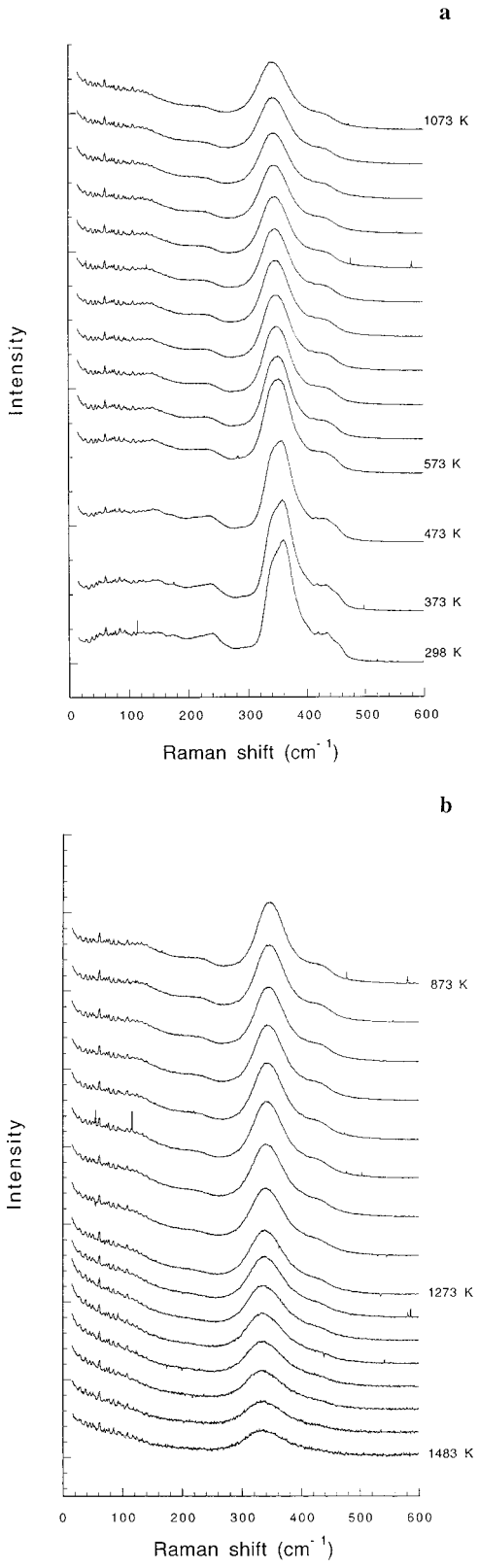

Figure 3. Raman spectra of $Ca_3(VO_4)_2$, corrected for thermal emission, in the low wavenumber region as a function of temperature: (a) 298−1073 K; (b) 873−1483 K. The spectra in the 573−1273 and 1273−1483 K temperature ranges were collected every 50 and 30 K, respectively.

of the observed Raman bands, are shown in Figures 2−4. The procedure for analyzing the temperature evolution of the Raman spectra was based on a multi-Lorentzian function supplemented with a Lorentzian-type shape for the Rayleigh elastic scattering. Initially, the room-temperature Raman spectrum (Figure 1) was approximated with the smallest number of bands to obtain the best fit (Table 1). Then, this result was used

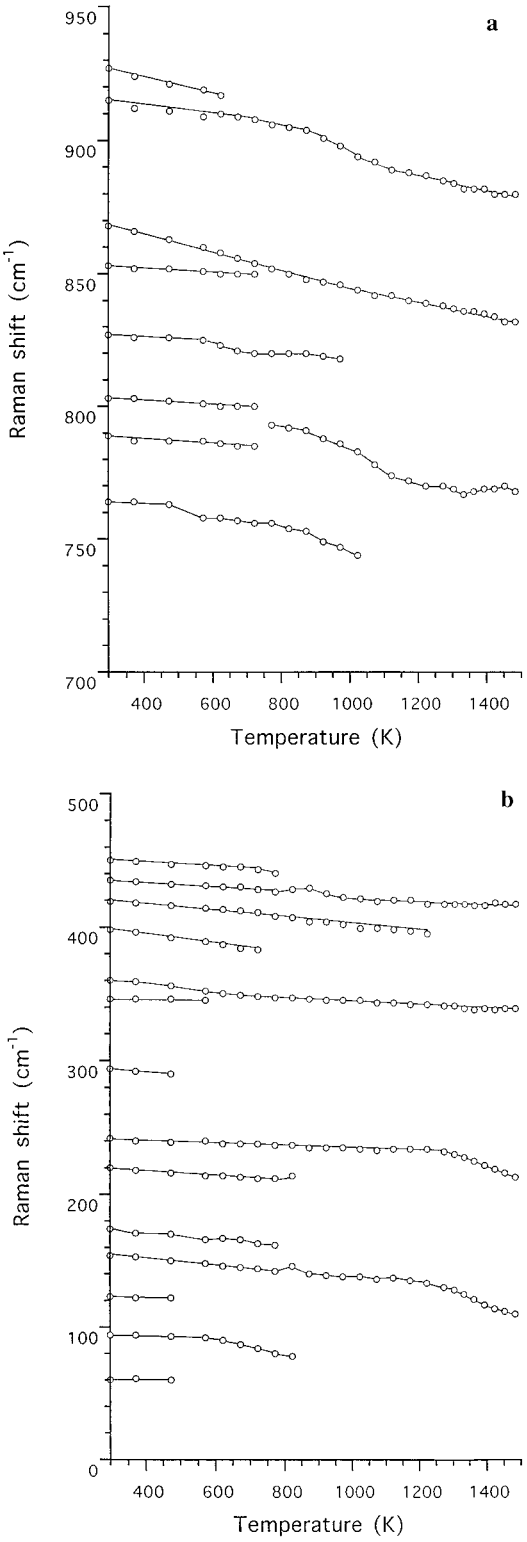

Figure 4. Temperature shift of the observed Raman bands in $Ca_3(VO_4)_2$ in the (a) 950−700 cm^{-1} and (b) 500−0 cm^{-1} wavenumber regions. The lines are guides for the eyes.

as a starting point for high-temperature data (Figures 2 and 3) with subsequent removal of weak and not well-defined bands, in the case when the quality of the fit with a smaller number of Lorentzian bands was comparable (the χ^2 parameter). Afterward, the fitting was reversed, starting with the smallest number of bands for the highest temperature spectrum (1483 K) and occasionally adding new bands to the fit at decreasing temperatures. Such a procedure for fitting Raman spectra as a function of temperature was necessary to obtain consistent results[23] (Figure 4).

An examination of the Raman spectra at high temperatures reveals that the major changes in the structure of $Ca_3(VO_4)_2$ occur in a broad temperature range below approximately 800 K (Figures 2−4). It is evidenced by merging or vanishing of some of the bands and an increase in intensity of the bands at the V−O stretching mode region. It is seen in Table 1 that the bands that are merging (or that cannot be resolved unambiguously into two components in unpolarized Raman spectra) at temperatures about 800 K are mainly the pairs of the A_1 and E symmetry types. It is seen from symmetry analysis and distribution of the internal modes of the tetrahedral ions at C_3 and C_1 sites that the internal modes of the VO_4^{3-} ions at the C_1 sites are mostly affected by increasing site symmetry to the higher-fold one, due to a smaller number of equivalent tetrahedral ions in the unit cell. It is also seen from Figure 4 that such high-temperature behavior of the predominantly internal modes is accompanied by vanishing of some of the low-wavenumber bands at about 500 K. Upon further heating above 800 K, there are no major changes in the temperature dependence of Raman spectra. At the vicinity of the ferroelectric phase transition at $T_c = 1383$ K[1] three bands can be resolved in the V−O bond stretching region, in agreement with the symmetry analysis for the $R\bar{3}m$ palmierite structure. The ferroelectric-paraelectric phase transition in $Ca_3(VO_4)_2$ is marked by the gradual change in the temperature dependence of two bands at the low-wavenumber region with no other significant changes at this temperature range. It is also noticeable that no soft modes are observed in the entire temperature range studied here. The analysis of the temperature dependence of band intensities and widths was not performed in a quantitative way due to a relatively large overlap of the bands in unpolarized Raman spectra, additionally broadened at high temperatures.[23,34] However, it is seen in Figures 2 and 3 that while all the bands in the 500−0 cm^{-1} wavenumber range decrease in their intensity, the bands at about 850 cm^{-1} increase in their intensity up to about 773 K. Such an effect is opposite to what is expected for the temperature dependence of the first-order Raman scattering studied here.[35] Through the presence of the term due to a thermal activation of the first-order phonons in the Bose−Einstein statistics, the intensity of the first-order Raman scattering should diminish exponentially with increasing temperature.

The temperature dependence of Raman features in $Ca_3(VO_4)_2$ below 800 K could be interpreted as a result of an increase in the local symmetry of the VO_4^{3-} ions. The number of the observed bands in the V−O stretching region at the vicinity of that temperature is not in agreement with the predicted one for the ideal palmierite structure. It could be related to the existence of an intermediate between the distorted $R3c$ structure at room temperature and the ideal $R\bar{3}m$ palmierite structure above T_c. Such intermediate structure would have

(34) Chan, S. S.; Wachs, I. E.; Murrell, L. L.; Wang, L.; Hall, W. K. *J. Phys. Chem.* **1984**, *88*, 5831.
(35) Reissland, J. A. *The Physics of Phonons*; John Wiley & Sons Ltd.: London, 1973.

all the VO_4^{3-} ions at the nonequivalent sites with average 3-fold symmetry. However, the high-temperature Raman data in this study do not provide any information on the bulk symmetry of the unit cell.

The spectral changes observed below 850 K are in agreement with the pyroelectric anomalies and the presence of a diffuse maximum in the temperature dependence of the dielectric constant[1] and the anomalies in electronic thermal emission spectra.[3] The increase of Raman intensity to about 773 K could mean that the Raman activity is enhanced by strong amplification of the electronic susceptibility modulation, which is the physical origin of Raman scattering. It means then that the dielectric and thermal emission anomalies have a common origin associated with the changes in the electronic structure of the incommensurate phase of $Ca_3(VO_4)_2$.[3,22] Such structural and electronic transformations due to ascent of local symmetry of the VO_4^{3-} ions in $Ca_3(VO_4)_2$ are occurring without elastic anomalies at this temperature range, as measured with Brillouin spectroscopy.[22]

The lack of soft-mode behavior in $Ca_3(VO_4)_2$ in the entire temperature range studied here is important to understand the nature of the observed phase transitions. The displacive transitions are associated with the soft mode, i.e., the mode with its wavenumber rapidly tending to zero as the phase transition is approached.[29] When the soft mode is absent, the phase transition is of the order−disorder character. On the basis of the selection rules for $R3c$ ferroelectric and $R\bar{3}m$ paraelectric phases, the ferroelectric soft mode has A_1 symmetry type.[27−29] The corresponding soft mode in the paraelectric phase is of the A_{2u} type, which is infrared, but not Raman, active. However, none of the A_1 modes, identified in a single-crystal study at room temperature (Table 1), tends rapidly to zero both in the 500−800 K temperature range and at $T_c = 1383$ K (Figures 2−4). It strongly suggests that the phase transitions in $Ca_3(VO_4)_2$ are of the order−disorder character, associated with an increase of local symmetry of the VO_4^{3-} tetrahedral units, as probed with Raman spectroscopy. Additionally, the absence of the elastic anomalies[22] at temperatures up to 840 K could be a sign of second-order character for the phase transition at this temperature range. However, the data on the volumetric or elastic behavior of $Ca_3(VO_4)_2$ at $T_c = 1383$ K are not available yet.

The results of this study should be compared with what is known about phase transitions in other compounds with the palmierite-type structure.[3,4,36−44] Such a comparison should serve as an indirect source of information on the nature and mechanism of the phase transitions in $Ca_3(VO_4)_2$. It is especially important for the case of Raman spectroscopy, which is quite sensitive to probe the transformations of the internal modes of molecular ions but does not provide sufficient information on the lattice oscillations. For that instance, the high temperature γ form of $Pb_3(VO_4)_2$ ($R\bar{3}m$) transforms into two monoclinic ferroelastic β ($P2_1/c$ space group) and ferroelectric α (A_2 space group) phases at 373 and 273 K, respectively.[36,37] Through these transitions, associated with strong volumetric discontinuities, the VO_4^{3-} tetrahedra remain rigid and the interlayer $Pb_{(2)}$ atoms are shifted from their ideal positions (C_{3v}) to accommodate the steric effects due to a changing delocalization of their electronic lone pairs.[36] However, no soft mode, associated with these structural changes, was detected in a Raman study.[38] The results of dielectric and dilatometric measurements suggest that the mechanism of the successive phase transitions in $Pb_3(VO_4)_2$ is of the order−disorder type.[39,40] The $Ca_{3-x}Pb_x(VO_4)_2$ system at ambient conditions consists of two solid solutions series.[4] The join with $0 \le x \le 1.45$ is isostructural with $Ca_3(VO_4)_2$ ($R3c$) and possesses lowered temperatures of a para-ferroelectric phase transition, $1213\ K \le T_c \le 1383$ K. The other series with $2.32 \le x \le 3$ is comprised of three different forms with their structures related to $Pb_3(VO_4)_2$. The transition temperature between the ferroelastic−antiferroelectric $P2_1/C$ form and the prototypic palmierite one ($R\bar{3}m$) is observed at room temperature for $x = 2.75$. However, nothing is known about the effect of the Pb substitution on the dielectric anomalies in $Ca_3(VO_4)_2$ at the 500−800 K temperature range. Overall, the mechanism of the phase transitions in $Ca_3(VO_4)_2$ could be similar to that in $Pb_3(VO_4)_2$. In both materials, there is no soft mode observed and Raman scattering well documents the changes in the local symmetry of the VO_4^{3-} ions. However, in analogy to $Pb_3(VO_4)_2$, it rather shifts of the $Ca_{(2)}^{2+}$ ions from their ideal positions at temperatures below $T_C = 1383$ K that account for the symmetry changes of the lattice and observed dielectric and electronic anomalies in $Ca_3(VO_4)_2$. The VO_4^{3-} units, rigid through these transformations, change their local symmetry in response to shifting interlayer cations.

Although the solid solution series in the $Ca_3(VO_4)_2$−$Ca_3(PO_4)_2$ system is known,[3] the effect of the P substitution in $Ca_3(VO_4)_2$ on the ferroelectric properties has not been studied yet. It would be quite interesting to investigate these properties and mechanism of phase transistions in correlation with the chemical substitution at the tetrahedral sites. For example, $Pb_3(PO_4)_2$ and $Pb_3(P_{0.77}As_{0.23}O_4)_2$ undergo a ferroelastic transition between para ($R\bar{3}m$ space group) and ferro ($C2/c$ space group) phases.[41−44] This phase change originates from shifts of the $Pb_{(1)}$ atoms from the C_3 axis of the D_{3d} site, along three directions of the C_2 axes. It is first order for $Pb_3(PO_4)_2$ and becomes second order whenever phosphorus is partially substituted by arsenic in the $Pb_3(PO_4)_2$−$Pb_3(AsO_4)_2$ system. In the case of $Pb_3(PO_4)_2$, there occurs an intermediate between the $R\bar{3}m$ and $C2/c$ phases, in which the shifts of the $Pb_{(1)}$ atoms in the three possible directions are equivalent. It can then be concluded that the mechanism of phase transitions in the compounds with the palmierite structure is depend-

(36) Kiat, J. M.; Gamier, P.; Pinot, M. *J. Solid State Chem.* **1991**, *91*, 339.
(37) Kasatani, H.; Umeki, T.; Terauchi, H. *J. Phys. Soc. Jpn.* **1992**, *61*, 2309.
(38) Kuok, M. H.; Lee, S. C.; Tong, S. H.; Midorikawa, M.; Ishibashi, Y. *Solid State Commun.* **1988**, *66*, 1035.
(39) Midorikawa, M.; Kashida, H.; Sawada, A.; Ishibashi, Y. *J. Phys. Soc. Jpn.* **1980**, *49*, 1095.
(40) Midorikawa, M.; Kashida, H.; Ishibashi, Y. *J. Phys. Soc. Jpn.* **1981**, *50*, 1592.
(41) Bismayer, U.; Salje, E. *Acta Crystallogr.* **1981**, *A37*, 145.
(42) Salje, E.; Bismayer, U. *Phase Transform.* **1981**, *2*, 15.
(43) Salje, E.; Yagil, Y. *J. Phys. Chem. Solids* **1996**, *57*, 1413.
(44) Salje, E. K. H. *Phase Transform.* **1992**, *37*, 83.

ent on the cation present at the tetrahedral sites, although it is the shift of intra- or interlayer cations that accounts for the symmetry and property changes. Thus, the chemical substitution at the tetrahedral sites should allow tuning of the nonlinear materials properties.

Acknowledgment. I thank Philippe Gillet for making his Raman instrument available for this study. I also acknowledge Paul McMillan for several insightful suggestions.

CM9705810